http://dx.doi.org/10.5755/j02.eie.33844 ELEKTRONIKA IR ELEKTROTECHNIKA, ISSN 1392-1215, VOL. 29, NO. 3, 2023

A New Method to Synthesise the Sinusoidal Oscillator Based on Series Negative Resistance-Capacitance and its Implementation Using a Single Commercial IC, LT1228

Worawut Kulapong[1], Winai Jaikla[1, *], Surapong Siripongdee[1], Roman Sotner[2], Peerawut Suwanjan[1], Amornchai Chaichana[1]

[1]*Department of Engineering Education, School of Industrial Education and Technology, King Mongkut's Institute of Technology Ladkrabang, Bangkok, 10520, Thailand*

[2]*Department of Radio Electronics, Faculty of Electrical Engineering and Communication, Brno University of Technology, Technicka 12, Brno, 616 00, Czechia*

64603094@kmitl.ac.th; [*]winai.ja@kmitl.ac.th; surapong.si@kmitl.ac.th; sotner@vut.cz; peerawut.su@kmitl.ac.th; amornchai.ch@kmitl.ac.th

***Abstract*—An alternative method for synthesising the sinusoidal oscillator based on series negative resistance-capacitance is presented in this paper. The proposed topology is constructed with the series negative resistance-capacitance circuit connected in parallel with a grounded resistor and capacitor. To validate the proposed method, a new grounded series negative resistance-capacitance simulator is also proposed as a subcircuit for synthesising the sinusoidal oscillator. The series negative resistance-capacitance simulator is based on a commercially available integrated circuit (IC), LT1228. The equivalent negative resistance and equivalent negative capacitance can be adjusted electronically using an external DC bias current. The sinusoidal oscillator that is synthesised using the proposed method consists of a single LT1228, two capacitors, and three resistors. The frequency and the condition of the oscillation are orthogonally adjusted. Also, the condition of oscillation is electronically controlled. The amplitude of the sinusoidal waveform is adjustable. In addition, the output voltage node of the proposed oscillator has a low impedance, which allows it to connect to other circuits without using an additional buffer. Both PSPICE simulation and experiment are used to validate the proposed circuits.**

***Index Terms*—LT1228; Negative capacitance simulator; Negative resistance simulator; Sinusoidal waveform.**

I. INTRODUCTION

Sinusoidal oscillators are crucial analogue circuits in numerous electrical and electronic engineering applications, including telecommunications, sound systems, measurement systems, instrumentation, and control systems [1]. In open literature, many methods have been proposed to synthesise the sinusoidal oscillators, e.g., based on integrator circuits [2], differentiator [3], first-order all-pass filter [4], frequency-dependent negative resistance (FDNR) simulator [5]. Classical LC sinusoidal oscillators, such as the Colpitts oscillator and the Hartley oscillator [6], are also synthesised by constructing an LC network with an amplifier.

The design of resistance, inductance, and capacitance simulators for use in place of passive components has been continuously proposed [7]–[17]. Simulators are often constructed from active and passive parts, including resistors and capacitors. However, the inductor is not preferred due to its size and expense [18]. Simulators for resistors and capacitors can be created in both positive and negative forms. Negative resistor and capacitor simulators are also utilised in a variety of applications. The employment of both negative and positive impedance elements permits the design of more complicated circuits, which can result in enhanced stability, higher efficiency, and a wider frequency tuning range. This can be especially beneficial in signal creation, filtering, and amplification applications that require steady oscillation with specified frequency response characteristics parasitic element rejection, sine wave oscillator, and impedance matching [19]–[26].

To develop high performance circuits with fewer passive and active components, active building blocks (ABBs) have become an important factor in the design of contemporary analogue signal processing systems. In the research literature, a large number of alternative designs for ABB have been proposed [27]. These circuits can be realised at the transistor level in bipolar junction transistor (BJT) and complementary metal oxide semiconductor (CMOS) technologies. However, most performance verification has been limited to simulation tools only because of the expensive cost of integrating these ABBs into an integrated circuit chip. The use of available integrated circuits (ICs) might be a cost-effective option for testing and other

Manuscript received 6 February, 2023; accepted 15 April, 2023.

This research is financially supported by the School of Industrial Education and Technology, King Mongkut's Institute of Technology Ladkrabang (KMITL) under Grant No. 2565-02-03-003.

applications [28], [29]. The LT1228 [30] is a widely used commercially available operational transconductance amplifier with electronically variable transconductance gain (g_m), which makes circuits based on the LT1228 easy to operate with a microcontroller or microcomputer [10].

The objective of this paper is to propose an alternative method for synthesising the sinusoidal oscillator using a series negative resistance-capacitance simulator connected in parallel with a grounded resistor and capacitor. The organisation of this paper is as follows. The proposed method, the basic concept of the commercially available LT1228 IC, the series negative resistance-capacitance simulator, and the proposed sinusoidal oscillator are described in Section II. The simulation results of the proposed series negative resistance-capacitance simulator and sinusoidal oscillator, as well as the experimental results of the sinusoidal oscillator, are shown in Section III. Finally, the conclusions are summarised in Section IV.

II. CIRCUIT DESCRIPTION

A. Synthetisation of Sinusoidal Oscillator Based on Series Negative Resistance-Capacitance

There have been several alternative approaches proposed as potential ways to synthesise the sine wave oscillator. In this paper, the synthesis makes use of the arrangement of the series negative resistance-capacitance (R_n and C_n) connected in parallel with the resistance and capacitance (R_2 and C_2) shown in Fig. 1. In practise, the series negative resistance-capacitance is an active circuit called the “simulator”. It can be constructed from the active device with a few passive elements. The following characteristic equation of the circuit shown in Fig. 1 is obtained as follows

$$s^2 + s\left(\frac{1}{C_2R_2} + \frac{1}{C_nR_n} - \frac{1}{C_2R_n}\right) + \frac{1}{C_nC_2R_nR_2} = 0. \qquad (1)$$

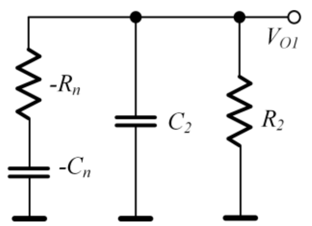

Fig. 1. Sinusoidal oscillator based on the series negative resistance-capacitance connected in parallel with resistance and capacitance.

From the characteristic equation shown in (1), the equations for the frequency of oscillation (FO) and condition of oscillation (CO) are as follows:

$$\text{FO}: \omega_0 = \sqrt{\frac{1}{C_nC_2R_nR_2}}, \qquad (2)$$

$$\text{CO}: 1 \geq \frac{R_n}{R_2} + \frac{C_2}{C_n}. \qquad (3)$$

It is clearly seen from (2) and (3) that FO and CO are not independently or orthogonally controlled. However, if the parameters in the negative resistance and capacitance values are coupled, the FO and CO could be orthogonally adjusted. It will be shown in detail in the design step later.

B. Overview of the Active Element, LT1228

The LT1228 commercial IC from Linear Technology [30] is an eight-lead plastic dual in-line package (PDIP) package. It features eight terminals, including two input terminals, three output terminals, one terminal for the DC bias current for electronically adjusting the transconductance (g_m), and the remaining two terminals for a wide range of power supply voltage (±2 V to ±15 V).

Figure 2(a) shows the electrical symbol of the LT1228. This active device consists of an operational transconductance amplifier (OTA) and a current feedback amplifier (CFA), and its equivalent circuit is depicted in Fig. 2(b). The matrix equation as shown in (4) will be used to calculate the ideal terminal characteristic relation that exists between voltage and current for the LT1228

$$\begin{pmatrix} I_{V+} \\ I_{V-} \\ I_y \\ V_x \\ V_w \end{pmatrix} = \begin{pmatrix} 0 & 0 & 0 & 0 & 0 \\ 0 & 0 & 0 & 0 & 0 \\ g_m & -g_m & 0 & 0 & 0 \\ 0 & 0 & 1 & 0 & 0 \\ 0 & 0 & 0 & R_T & 0 \end{pmatrix} \begin{pmatrix} V_+ \\ V_- \\ V_y \\ V_x \\ I_w \end{pmatrix}. \qquad (4)$$

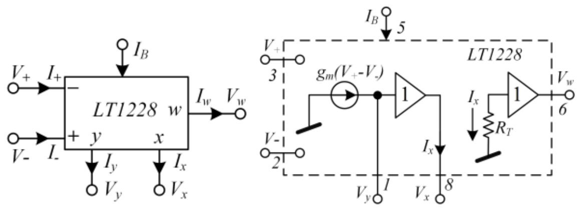

(a) (b)

Fig. 2. LT1228: (a) Symbol; (b) Equivalent circuit [10].

As shown in Fig. 2, the transconductance is electronically adjustable by DC supply at the bias current, I_B (pin five). The relationship between g_m, I_B, and thermal voltage can be derived using (5)

$$g_m = \frac{I_B}{3.87V_T}. \qquad (5)$$

From (5), V_T is the thermal voltage and the g_m at room temperature is around $g_m = 10I_B$.

C. Proposed New Grounded Series Negative Resistance-Capacitance Simulator

As shown in Fig. 3(a), the proposed grounded series negative resistance-capacitance simulator is capable of electrical control through the I_B. It uses a single commercial IC called “LT1228” and is constructed using a single resistor and a single grounded capacitor. The input impedance of the proposed grounded series negative resistance-capacitance simulator can be obtained from (6)

$$Z_{in} = \frac{v_{in}}{i_{in}} = -\frac{1}{g_m} - \frac{1}{sC_1R_1g_m}. \qquad (6)$$

The value of the equivalent negative capacitance, which is denoted by C_{eq}, and the value of the equivalent resistance, which is denoted by R_{eq}, can be derived using the method described in more detail in (7) and (8):

$$C_{eq} = -g_m C_1 R_1, \tag{7}$$

$$R_{eq} = -\frac{1}{g_m}. \tag{8}$$

Referring to (6) illustrates a significant advantage of this design, which is that the value of the equivalent resistance, as well as the value of the equivalent capacitance, may be electronically adjusted by the bias current.

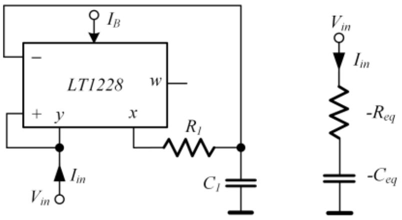

(a) (b)

Fig. 3. (a) Proposed grounded series negative resistance-capacitance simulator; (b) Equivalent circuit.

D. Series Negative Resistance-Capacitance-Based Sinusoidal Oscillator with Amplitude Controllability

Based on the principle shown in Fig. 1, the oscillator is constructed from the series negative resistance-capacitance connected in parallel with the grounded resistance and capacitance. Using the grounded series negative resistance-capacitance simulator shown in Fig. 3(a) and connecting the grounded resistor (R_2) and capacitor (C_2) to the input impedance node, it yields the proposed sinusoidal oscillator as depicted in Fig. 4(a). It is seen that the proposed sinusoidal oscillator is simple and consists of an active element, LT1228. The resistor R_3 connected between the x and w terminals of LT1228 is used to adjust the amplitude of the output voltage, V_{O2}. The characteristic equation of the sinusoidal oscillator shown in Fig. 4(a) can be derived from (9) in the following manner

$$s^2 + s\left(\frac{1}{C_1 R_1} + \frac{1}{C_2 R_2} - \frac{g_m}{C_2}\right) + \frac{1}{C_1 C_2 R_1 R_2} = 0. \tag{9}$$

Based on the characteristic equation shown in (9), the equations for FO and CO are presented in (10) and (11):

$$\text{FO}: \omega_0 = \sqrt{\frac{1}{C_1 C_2 R_1 R_2}}, \tag{10}$$

$$\text{CO}: 1 \geq \frac{1}{g_m R_2} + \frac{C_2}{C_1 R_1 g_m}. \tag{11}$$

If $C_1 = C_2$ is defined, the FO and CO are given by:

$$\text{FO}: \omega_0 = \frac{1}{C}\sqrt{\frac{1}{R_1 R_2}}, \tag{12}$$

$$\text{CO}: 1 \geq \frac{R_1 + R_2}{g_m R_1 R_2}. \tag{13}$$

Using (12) and (13), FO can be controlled separately from CO by using C_1 and C_2. In addition to this, use (13) with g_m to set CO in a manner that may be controlled independently of FO. However, to ensure that the circuit is in compliance with CO, capacitors C_1 and C_2 will need to have the required matching between them. From the oscillator shown in Fig. 4(a), the voltage ratio of V_{O2} and V_{O1} can be found in (14)

$$\frac{V_{O2}}{V_{O1}} = 1 + \frac{sC_1 R_3}{sC_1 R_1 + 1}. \tag{14}$$

At the oscillation frequency, if $R_1 = R_2$ and $C_1 = C_2$, the magnitude of the voltage ratio for V_{O2} and V_{O1} is found as follows

$$\left|\frac{V_{O2}}{V_{O1}}\right| = \frac{1}{\sqrt{2}}\sqrt{\left(\frac{R + R_3}{R}\right)^2 + 1}. \tag{15}$$

Equation (15) indicates that the magnitude of V_{O2} is adjusted via R_3 without affecting the FO and CO. Furthermore, the output voltage node (V_{O2}) has a low impedance, which allows it to connect to other circuits without the need for a voltage buffer.

Considering the parasitic elements of the nonideal circuit as shown in Fig. 4(b), there are parasitic resistances and capacitances between the high impedance terminals and ground. These parasitic capacitances and resistances include C_+, C_-, C_y, R_+, R_-, and R_y. To evaluate the influences of these parasitic elements on oscillator performance, the circuit in Fig. 4(b) is considered. The FO and CO with parasitic element influences are, respectively, given by

$$\omega_0 = \sqrt{\frac{1 - \frac{g_m R_1 R_2}{R_-} + \frac{R_2}{R_y} + \frac{R_1 R_2}{R_- R_y} + \frac{R_1}{R_-} + \frac{R_2}{R_+} + \frac{R_1 R_2}{R_- R_+}}{C_1 C_2 R_1 R_2}} \tag{16}$$

and

$$1 \geq \frac{1}{g_m R_1 R_2 (C_1 + C_-)}\left[\begin{array}{l} C_1 R_1 + C_2 R_2 + C_- R_1 + \frac{R_1 R_2}{R_-}\left(C_2 + C_+ + C_y\right) + \\ + R_1 R_2 \left(C_1 + C_-\right)\left(\frac{1}{R_+} + \frac{1}{R_y}\right) + C_+ R_2 + C_y R_2 \end{array}\right]. \tag{17}$$

It is obvious that the parasitic impedances in LT1228 have an impact on FO and CO. Also, it is found that the control of CO by g_m as shown in (17) will slightly affect FO as shown in (16) due to parasitic resistance, R_-.

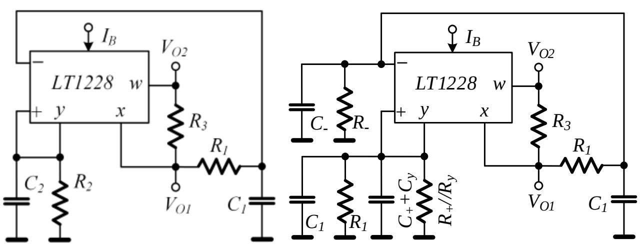

(a) (b)

Fig. 4. Proposed sinusoidal oscillator based on series negative RC simulator: (a) Ideal circuit; (b) Including parasitic elements.

III. Simulation and Experimental Results

A. Simulated Grounded Series Negative RC Simulator Using PSPICE

To illustrate the functionality of the proposed grounded series negative resistance-capacitance simulator circuit depicted in Fig. 3(a) and to conduct a performance evaluation on it, the PSPICE simulation was carried out. The level 5 macro model of LT1228 IC in the PSPICE library was used. As shown in Fig. 3(a), the proposed circuit was constructed using a commercially available IC, LT1228 and a single resistor and single grounded capacitor. The proposed circuit was supplied with DC voltages ±5 V. Other active and passive elements were set as follows: g_m = 2 mS (I_B = 206 μA), capacitor C_1 = 1 nF, and resistor R_1 = 1 kΩ. Based on the equivalent negative capacitance and equivalent negative resistance described in (7) and (8), the calculated equivalent negative capacitor is C_{eq} = -2.059 nF and the calculated equivalent negative resistance is R_{eq} = -485.667 Ω. As shown in Fig. 5, the frequency responses and phase of input impedance were produced using circuit proposed in Fig. 3(a).

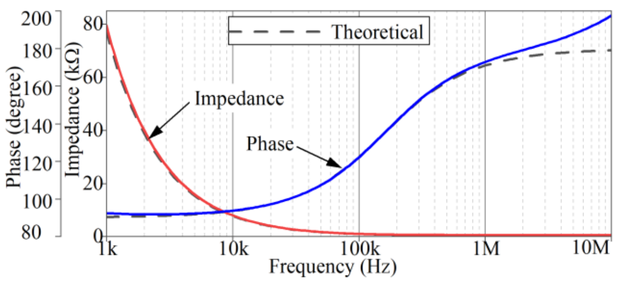

Fig. 5. The magnitude and phase response of the series negative RC simulator.

The simulation results indicate that the proposed circuit can work as a series of negative resistances and negative capacitances as expected. However, Fig. 5 is a frequency response graph showing how the phase value of the proposed circuit deviates from the theoretical value in the low frequency range (below 3 kHz) and in the high frequency range (over 1 MHz), it deviates from the theoretical value due to tracking error and parasitic parameters such as parasitic resistance and parasitic capacitances of LT1228. Figure 6 illustrates the magnitude frequency response of the input impedance for various I_B values.

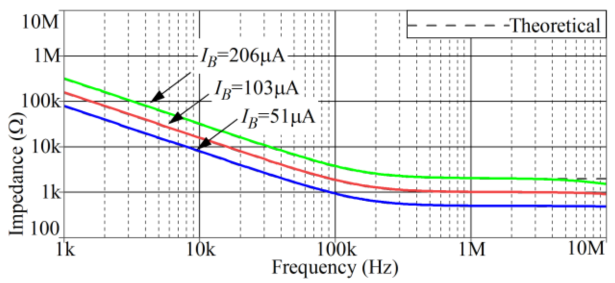

Fig. 6. The magnitude response when perform electronically tuneable in various I_B.

The result of the simulation in Fig. 6 demonstrates that the negative resistance and capacitance are electronically tuned in compliance with the specified by (7) and (8). To examine the effect of the passive component tolerance on the proposed simulator performances, the Monte Carlo analysis of the proposed negative is carried out. In this simulation, the value of passive component is varied by 5 % uniformly, while the active element is the same as stated. After 150 runs, the magnitude and phase responses of the input impedance of the proposed simulator are shown in Fig. 7.

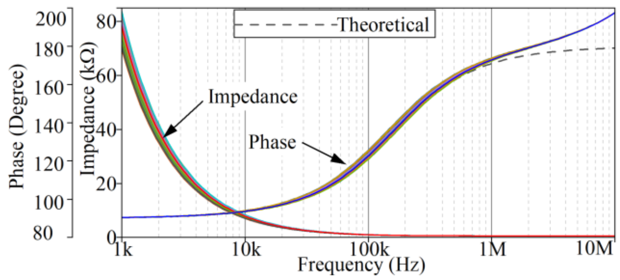

Fig. 7. A Monte Carlo analysis result with 150 runs for 5 % passive component tolerance.

B. Sinusoidal Oscillator Based on Grounded Series Negative RC Simulator Using PSPICE

PSPICE simulation was carried out to evaluate and demonstrate a performance of the proposed sinusoidal oscillator based on a grounded series negative resistance-capacitance circuit. The proposed oscillator was supplied by DC voltages ±5 V. To illustrate the proper operation of the sinusoidal oscillator, the CO in (13) must be fulfilled. The DC bias current I_B was set to 206 μA to obtain g_m = 2 mS, capacitor C_1 = 1 nF, C_2 = 1 nF, resistor R_1 = 1 kΩ, R_2 = 1 kΩ, and R_3 = 1 kΩ. The expected frequency of oscillation is 159.15 kHz according to (12). The simulation determined that the oscillation frequency (f_{osc}) is 159 kHz, as shown in Fig. 8(a), and the output spectrum of sinusoidal waveform with total harmonic distortion (*THD*) = 0.418 % is shown in Fig. 8(b).

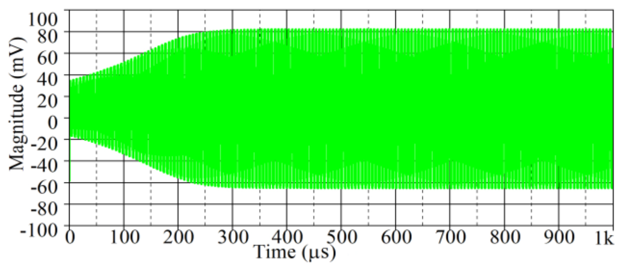

(a)

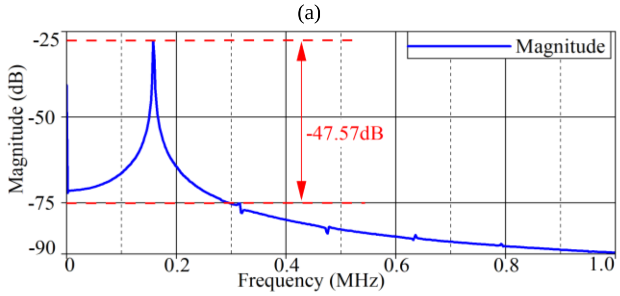

(b)

Fig. 8. (a) Sinusoidal waveform (f_{osc} = 159 kHz) at node V_{O1}; (b) Output spectrum of the sine wave at node V_{O1}.

As anticipated, the results reveal that the proposed oscillator depicted in Fig. 4(a) is functional. The frequency of the oscillator in the proposed circuit deviates from its theoretical value by 0.1 % due to tracking error and parasitic factors such as parasitic resistance and parasitic capacitances of LT1228 as shown in Fig. 4(b).

The oscillation frequency for various capacitors values is shown in Fig. 9. It is found that C_1 and C_2 are tuned to produce the oscillation frequency as depicted in (12). With C_1 and C_2 being 1 nF, the simulated frequency is 159 kHz (0.1 % error). When C_1 and C_2 are set to 0.8 nF, the simulated frequency is 199 kHz (0.03 % error). Finally, set both capacitor values to 0.6 nF, the simulated frequency is 264 kHz, which deviates by 0.47 % from its theoretical value. As analysed in (15), the magnitude of the sinusoidal waveform at node V_{O2} depends on R_3. So, the simulation was carried out by changing various resistor R_3 values as the result depicted in Fig. 10. The simulation result demonstrates that R_3 has been changed to provide the magnitude of the difference without affecting FO and CO as indicated in (15).

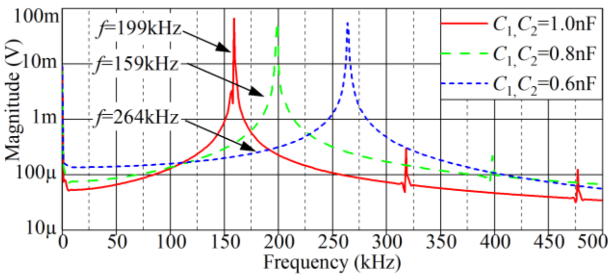

Fig. 9. The oscillation frequency at node V_{O1} by various values of $C_1 = C_2$.

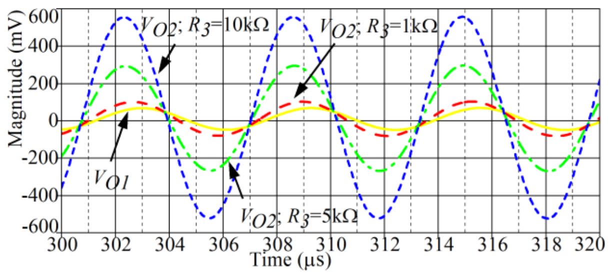

Fig. 10. The output gain at node V_{O2} by various value of R_3.

C. Experiment Result of the Proposed Sinusoidal Oscillator

The purpose of the experiment was to prove the performance of the proposed sinusoidal oscillator based on a grounded series negative resistance-capacitance simulator. To illustrate the proper operation of the sinusoidal oscillator, the proposed circuit was supplied by dual DC ±5 V from GW INSTEK Model GPS-3303. The oscilloscope and digital multimeter by Keysight DSOX-D1102G and RICHMETERS Model RM303 were used, respectively. To acquire g_m = 2 mS, a bias resistor with a value of 17.859 kΩ was connected between the pin 5 terminal of LT1228 and the ground to bias the I_B. With this biasing, the amount of bias current I_B was obtained to 206 µA. The capacitor C_1 was set at 1 nF while resistor R_1 was set at 1 kΩ. To fulfil the oscillation, the conditional of oscillation in (11) must be achieved. The capacitor C_2 value was determined to be 1 nF, while the resistor R_2 value was found to be 1 kΩ. According to the information provided, the expected frequency of oscillation (FO) is 159.15 kHz according to (10). Figure 11 illustrates the experimental setup in detail.

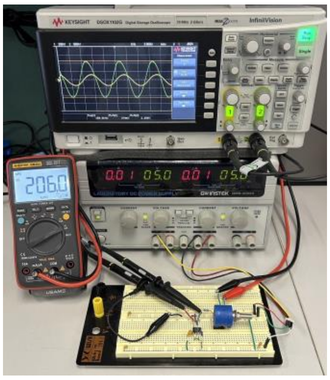

Fig. 11. Experimental setup for the sinusoidal oscillator.

The results of the experiments presented in Fig. 12(a) and Fig. 12(b) demonstrate that the principle shown in Section II-A is available and the proposed circuit can produce a sinusoidal waveform with a frequency of 171.8 kHz at output voltage node V_{O1} with 0.60 % total harmonic distortion (THD). Although this frequency is relatively close to the theoretical value of 159.15 kHz, it differs from this value by 7 %. Resistors R_3 = 10 kΩ have been added to adjust the amplitude of the output voltage V_{O2}.

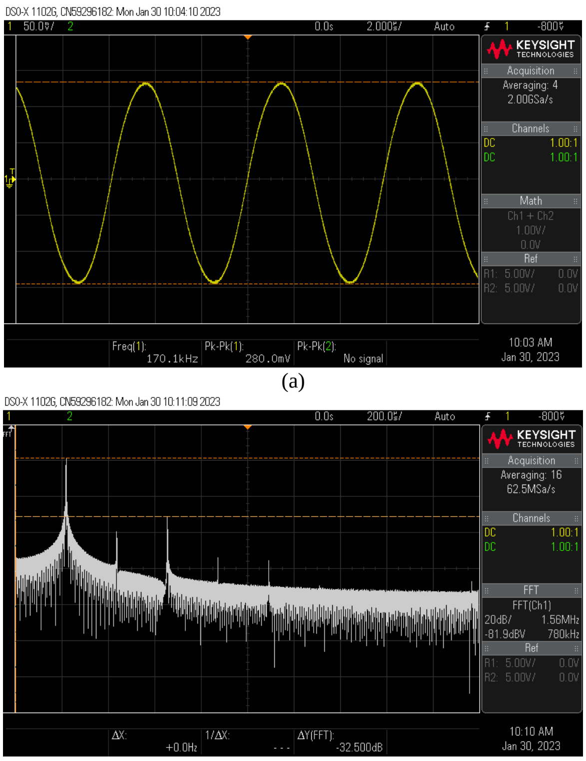

(a)

(b)

Fig. 12. (a) Sinusoidal output voltage waveform at V_{O1}; (b) Sinusoidal output spectrum at V_{O1} with 0.604 % THD.

The experimental result determined that the oscillation waveform at node V_{O2} with oscillation frequency (f_{osc}) is 171.6 kHz, as shown in Fig. 13(a), and Fig. 13(b) depicts the output spectrum of sinusoidal output V_{O2} with 0.81 % THD. The voltage gain of the sinusoidal output waveforms of V_{O2} and V_{O1} is 8.33, which deviates by 3 % from its theoretical gain.

(a) (b)

Fig. 13. (a) Sinusoidal output voltage waveform V_{O2} when R_3 = 10 kΩ; (b) Output spectrum V_{O2} with 0.806 % THD.

IV. DISCUSSION AND COMPARISON

Table I compares the proposed negative simulator with those negative simulators [19]–[26]. The proposed circuit can function as a negative capacitor in series with a negative resistor, while lossless negative capacitance simulators are proposed in [19]–[22], [24]–[26]. The simulator proposed in [23] functions as a negative inductor in series with a negative resistor. Most of them use only one ABB; however, more than one ABB is required for the simulators in [20], [24]–[26]. The proposed circuit uses one commercially available integrated circuit, but the circuits in [19], [21]–[25] need more than one IC for practical implementation. In [21], [24], and [25], electronic control is not available. In addition, by connecting only one resistor and one capacitor to the input node of the proposed negative simulator based on the new concept depicted in Fig. 1, a simple sinusoidal oscillator is achieved, but the negative simulators proposed in [19]–[26] are not available for this synthesis.

TABLE I. COMPARISON OF THE PROPOSED NEGATIVE SIMULATOR AND OTHER WORKS.

Ref.	**Negative simulator category**	**No. of ABB**	**No. of commercial IC**	**No. passive device**	**Electronic tune**	**Availability to be synthesised in the sinusoidal oscillator based on a series negative RC depicted in Fig. 1**
[19]	−C	1 VDTA	-	3	yes	no
[20]	−C	1 CFOA, 2 OTA	3	1	yes	no
[21]	−L and −C	1 CFA	1	3	no	no
[22]	−L, −C and −R	1 VCII, 1 OTA	2	2	yes	no
[23]	−L series with −R	1 VDCC	-	2	yes	no
[24]	−C	1 OTRA, 1 VF	2	4	no	no
[25]	−C	2 VCII	2	3	no	no
[26]	−C	2 CFTA	-	1	yes	no
Proposed	−C series with −R	1 LT1228	1	2	yes	yes

V. CONCLUSIONS

This paper presents a new method for synthesising a second-order sinusoidal oscillator based on a series negative resistance-capacitance circuit. The principle for generating a sine wave is formed from the series negative RC connected in parallel with the grounded resistor and capacitor. The new series negative RC simulator has also been proposed as the subcircuit for forming the sinusoidal oscillator. The proposed simulator with electronic controllability is realised with a single LT1228, R_1 and C_1. By connecting R_2 and C_2 in parallel to the series negative RC simulator based on the proposed principle, a sinusoidal oscillator is achieved with electronic control of the oscillation condition. The frequency of oscillation can be adjusted by simultaneously changing C_1 and C_2 without affecting the oscillation condition. By connecting R_3 between the *x* and *w* terminals of LT1228, the amplitude of the sinusoidal waveform at node V_{O2} is adjustable without affecting the frequency or condition of oscillation. The performance of the proposed oscillator is verified by PSPICE simulation and hardware experimentation with ±5 V voltage supplies. The oscillation frequencies obtained from the simulation and experiment are 159 kHz (0.53 % THD) and 171.6 kHz (0.81 % THD), respectively.

CONFLICTS OF INTEREST

The authors declare that they have no conflicts of interest.

REFERENCES

[1] A. S. Sedra and K. C. Smith, *Microelectronic Circuits*, 3rd ed. Philadelphia: Saunders College Pub., 1991.

[2] A. M. Soliman, "Transformation of oscillators using Op Amps, unity gain cells and CFOA", *Analog Integrated Circuits and Signal Processing*, vol. 65, pp. 105–114, 2010. DOI: 10.1007/s10470-010-9458-8.

[3] R. Nandi, S. K. Sanyal, and T. K. Bandyopadhyay, "Single CFA-based integrator, differentiator, filter, and sinusoid oscillator", *IEEE Transactions on Instrumentation and Measurement*, vol. 58, no. 8, pp. 2557–2564, 2009. DOI: 10.1109/TIM.2009.2014625.

[4] A. U. Keskin and D. Biolek, "Current mode quadrature oscillator using current differencing transconductance amplifiers (CDTA)", *IEE Proceedings - Circuits Devices and Systems*, vol. 153, no. 3, pp. 214–218, 2006. DOI: 10.1049/ip-cds:20050304.

[5] R. Nandi, K. Mathur, and P. Venkateswaran, "Electronically tunable immittances with applications to LP, BP, HP filter and VCO implementation", *International Journal of Electronics Letters*, vol. 9, no. 1, pp. 65–75, 2021. DOI: 10.1080/21681724.2019.1672800.

[6] M. K. Kazimierczuk and D. Murthy-Bellur, “Synthesis of LC sinusoidal oscillators”, *International Journal of Electrical Engineering Education*, vol. 49, no. 1, pp. 26–41, 2012. DOI: 10.7227/IJEEE.49.1.3.

[7] B. C. Nagar and S. K. Paul, “Lossless grounded admittance simulator using OTRA”, *Analog Integrated Circuits and Signal Processing*, vol. 106, pp. 649–659, 2021. DOI: 10.1007/s10470-019-01410-4.

[8] D. Agrawal and S. Maheshwari, “Electronically tunable grounded immittance simulators using an EX-CCCII”, *International Journal of Electronics*, vol. 107, no. 10, pp. 1625–1648, 2020. DOI: 10.1080/00207217.2020.1729421.

[9] R. Sotner, J. Jerabek, N. Herencsar, L. Langhammer, J. Petrzela, and T. Dostal, “Methods for extension of tunability range in synthetic inductance simulators”, *Elektronika ir Elektrotechnika*, vol. 24, no. 3, pp. 41–45, 2018. DOI: 10.5755/j01.eie.24.3.20976.

[10] S. Siripongdee and W. Jaikla, “Electronically controllable grounded inductance simulators using single commercially available IC: LT1228”, *AEU - International Journal of Electronics and Communications*, vol. 76, pp. 1–10, 2017. DOI: 10.1016/j.aeue.2017.03.018.

[11] R. Senani and D. R. Bhaskar, “New lossy/loss-less synthetic floating inductance configuration realized with only two CFOAs”, *Analog Integrated Circuits and Signal Processing*, vol. 73, pp. 981–987, 2012. DOI: 10.1007/s10470-012-9897-5.

[12] İ. Mamatov, Y. Özçelep, and F. Kaçar, “CNTFET based inductance simulator circuits employing single CFOA and its filter applications”, *Analog Integrated Circuits and Signal Processing*, vol. 111, pp. 235–242, 2022. DOI: 10.1007/s10470-022-02000-7.

[13] J. Ledvina and P. Horský, “A fully integrated digitally controllable grounded inductor simulator with a large inductance range for damping of ultrasonic transducers”, *Analog Integrated Circuits and Signal Processing*, vol. 102, pp. 125–130, 2020. DOI: 10.1007/s10470-019-01396-z.

[14] A. Singh, M. K. Jain, and S. Wairya, “Novel lossless grounded and floating inductance simulators employing a grounded capacitor based on CC-CFA”, *Journal of Circuits, Systems and Computers*, vol. 28, no. 6, pp. 1950093-1–1950093-12, 2019. DOI: 10.1142/S0218126619500932.

[15] F. Yuan, CMOS Active Inductors and Transformers: Principle, Implementation, and Applications. Springer Science & Business Media, 2008. DOI: 10.1007/978-0-387-76479-5.

[16] N. Herencsar, A. Lahiri, J. Koton, K. Vrba, and B. Metin, “Realization of resistorless lossless positive and negative grounded inductor simulators using single ZC-CCCITA”, *Radioengineering*, vol. 21, no. 1, pp. 264–272, 2012.

[17] E. Arslan, B. Metin, N. Herencsar, J. Koton, A. Morgul, and O. Cicekoglu, “High performance wideband CMOS CCI and its application in inductance simulator design”, *Advances in Electrical and Computer Engineering (AECE)*, vol. 12, no. 3, pp. 21–26, 2012. DOI: 10.4316/AECE.2012.03003.

[18] A. Thanachayanont and A. Payne, “CMOS floating active inductor and its application to band pass filter and oscillator design”, *IEE Proceedings - Circuits, Devices and Systems*, vol. 147, no. 1, pp. 42–48, 2000. DOI: 10.1049/ip-cds:20000053.

[19] P. B. Petrović, “Single VDTA-based lossless and lossy electronically tunable positive and negative grounded capacitance multipliers”, *Circuits, Systems, and Signal Processing*, vol. 41, pp. 6581–6614, 2022. DOI: 10.1007/s00034-022-02094-4.

[20] M. A. Al-Absi and M. T. Abuelma’atti, “A novel tunable grounded positive and negative impedance multiplier”, *IEEE Transactions on Circuits and Systems II: Express Briefs*, vol. 66, no. 6, pp. 924–927, 2019. DOI: 10.1109/TCSII.2018.2874511.

[21] Z. Xia, M. Li, and Z. Qi, “Realizing wideband negative inductor using current feedback amplifier”, *Microwave and Optical Technology Letters*, vol. 58, pp. 1723–1728, 2016. DOI: 10.1002/mop.29896.

[22] M. A. Al-Absi and A. Al-Khulaifi, “A novel tunable grounded positive and negative active inductor simulator and impedance multiplier”, *Arab. J. Sci. Eng.*, vol. 47, pp. 14983–14988, 2022. DOI: 10.1007/s13369-022-07338-8.

[23] F. Kacar, A. Yesil, S. Minaei, and H. Kuntman, “Positive/negative lossy/lossless grounded inductance simulators employing single VDCC and only two passive elements”, *AEU - International Journal of Electronics and Communications*, vol. 68, pp. 73–78, 2014. DOI: 10.1016/j.aeue.2013.08.020.

[24] D. R. Bhaskar, G. Mann, and P. Kumar, “OTRA-based positive/negative grounded capacitance multiplier”, *Analog Integrated Circuits and Signal Processing*, vol. 111, pp. 469–481, 2022. DOI: 10.1007/s10470-022-02032-z.

[25] V. Stornelli, L. Safari, G. Barile, and G. Ferri, “A new VCII based grounded positive/negative capacitance multiplier”, *AEU - International Journal of Electronics and Communications*, vol. 137, art. 153793, 2021. DOI: 10.1016/j.aeue.2021.153793.

[26] E. Özer, “Electronically tunable CFTA based positive and negative grounded capacitance multipliers”, *AEU - International Journal of Electronics and Communications*, vol. 134, art. 153685, 2021. DOI: 10.1016/j.aeue.2021.153685.

[27] D. Biolek, R. Senani, V. Biolkova, and Z. Kolka, “Active elements for analog signal processing: Classification, review, and new proposals”, *Radioengineering*, vol. 17, no. 4, pp. 15–32, 2008.

[28] W. Jaikla *et al.*, “Single commercially available IC-based electronically controllable voltage-mode first-order multifunction filter with complete standard functions and low output impedance”, *Sensors*, vol. 21, no. 21, p. 7376, 2021. DOI: 10.3390/s21217376.

[29] S. Maheshwari and M. S. Ansari, “Catalog of realizations for DXCCII using commercially available ICs and applications”, *Radioengineering*, vol. 21, no. 1, pp. 281–289, 2012.

[30] LT1228 - 100MHz Current Feedback Amplifier with DC Gain Control, Linear Technology. [Online]. Available: https://www.analog.com/media/en/technical-documentation/data-sheets/1228fd.pdf.